Some pluripotency-related genes, including *Nanog*, *Oct3/4*, and *Lin28a*, were upregulated in the Dox-withdrawn kidney tumor cells as compared to normal kidney tissue, although the expression levels of both *Nanog* and endogenous *Oct3/4* were significantly lower than that of pluripotent stem cells (Figures 3C and S3C). Conversely, other pluripotency-related genes, such as *Esrrb*, were not upregulated in these tumors (Figures 3C).

To further characterize Dox-withdrawn tumor cells, we sought to identify tumor-cell-specific markers. We found that *Lgr5* is specifically upregulated in Dox-withdrawn kidney tumor cells, but not in adult kidney tissues or pluripotent stem cells (Figure 3D). Increased expression of *Lgr5* was similarly observed in the transplanted secondary tumors (Figure S3D). Therefore, we established iPSC lines from OSKM-inducible MEFs containing *Lgr5-EGFP* reporter allele in which *Lgr5* expression can be visualized by enhanced green fluorescent protein (EGFP) (Barker et al., 2007). The established *Lgr5*-reporter iPSCs do not express EGFP in ESC culture conditions (Figure S3E). OSKM-inducible *Lgr5* reporter chimeric mice at 4 weeks of age were treated with the 7+/7− Dox regimen. Again, these mice developed Dox-withdrawn kidney tumors consisting of dysplastic cells (Figure 3E). The scattered EGFP signals were observed in kidney tumors (Figure 3E), and immunohistochemical analysis revealed that *Lgr5* is specifically expressed in part of Dox-withdrawn kidney tumor cells (Figures 3E and S3E). These findings indicate that Dox-withdrawn kidney tumors contain *Lgr5*-positive cells and that the *Lgr5* reporter allele is available to specifically identify the Dox-withdrawn kidney tumor cells that are distinct from fully reprogrammed pluripotent stem cells. Of note, some of the *Lgr5*-expressing tumor cells also expressed Oct3/4 and Lin28b in immunohistochemical analysis (Figures 3F and S3F), thus suggesting that *Lgr5*-expressing tumor cells share some characteristics with pluripotent stem cells. The fact that Dox treatment for longer than 8 days followed by Dox withdrawal often results in teratoma formation supports the notion that partial reprogramming toward pluripotent stem cells is involved in the development of Dox-withdrawn tumors (data not shown). Altogether, our findings indicate that *Lgr5*-expressing tumor cells are distinct from pluripotent stem cells but contain partially reprogrammed cells.

Failed Repression of ESC-Polycomb Targets in Dox-Withdrawn Tumors

In contrast to ESC-like activation observed for both the ESC-Core and ESC-Myc modules, the ESC Polycomb repressive complex (PRC) module was differentially expressed between Dox-withdrawn tumors and ESCs (Figure 4A). We found that a number of ESC-PRC targeted genes are not repressed in both kidney tumors and transplanted secondary tumors (Figures 4A, S4A, and S4B), indicating that the failed repression of ESC-PRC targets is associated with the development of Dox-withdrawn tumors. Consistent with the notion, more than one-forth of the upregulated genes in tumor cells as compared to ESCs (greater than 3-fold upregulation) were targets of PRC in ESCs (Mikkelsen et al., 2007) (Table S1). We also found that Dox-withdrawn kidney tumors express kidney-precursor-expressing genes such as *Six2*, *Eya1*, and *Lgr5* (Barker et al., 2012; Kobayashi et al., 2008) (Figures 4B and S4C). In particular, *Six2* and *Lgr5*, which are also PRC targets in ESCs (Mikkelsen et al., 2007), are specifically upregulated in both Dox-withdrawn kidney tumors and secondary tumors when compared to both normal kidney tissues and pluripotent stem cells (Figures 3D, 4B, S3D, and S4D). Chromatin immunoprecipitation (ChIP)-qPCR experiments confirmed decreased H3K27me3 levels at both *Six2* and *Lgr5* promoter regions in Dox-withdrawn tumors when compared with those in normal kidney tissues (Figure S4E). Failed repression of the ESC-PRC module was also detectable in unsuccessfully reprogrammed kidney cells in vitro, which were established by the transient expression of reprogramming factors in isolated kidney tubule cells in vitro (Figure S4F).

We next examined the kinetics of transcriptional changes during the development of the Dox-withdrawn tumors. Immunohistochemical analysis revealed that early dysplastic cells at day 7 coincide with transgene-expressing cells (Figure S4G). Taking advantage of florescence-linked transgene expression in our mice, we fluorescence-activated cell sorted mCherry-positive kidney cells in OSKM mice given Dox for 7 days (D7), isolating early dysplastic cells for gene expression analysis. Fluorescence-activated cell-sorted D7 LacZ-mCherry-expressing kidney cells were used as a control (Figure S4H). Decreased expression of proximal tubule cell markers was observed in the D7 OSKM cells as compared to D7 LacZ cells, suggesting that the loss of kidney cell identity occurs in early dysplastic cells (Figure S4I). In contrast, increased expression of ectopic stem/progenitor cell markers was not evident in D7 OSKM cells (Figure S4I). These findings suggest that remodeling of global transcriptional profiles toward a stem/progenitor-like state is specifically associated with transgene-independent, late dysplastic cells.

To investigate cell-of-origin effects on failed reprogramming, we next performed a microarray analysis for Dox-withdrawn liver tumors and compared the data with that of kidney tumors. As observed in kidney tumors, the liver tumors displayed failed repression of the ESC-PRC module, accompanied by activation of both the ESC-Core and Myc modules (Figure S4J; Table S1). Although derepressed PRC module genes in kidney tumors and liver tumors often overlapped (Figure S5A; Table S1), we found differentially derepressed PRC genes between kidney and liver tumors. Notably, such differentially derepressed PRC genes were associated with kidney and liver development, respectively. These findings suggest that failed PRC repression in Dox-withdrawn tumors may be associated with the activation of a developmental transcription

(F) Dox-withdrawn tumors express pluripotency-related proteins. Double immunofluorescence for Lin28b and GFP (Lgr5) revealed that the GFP-positive tumor cells also expressed Lin28b. Double immunofluorescence for Oct3/4 and GFP (Lgr5) showed that a subset of GFP-positive tumor cells expressed Oct3/4 in the nucleus. Scale bars, 20 μm.
See also Figure S3.

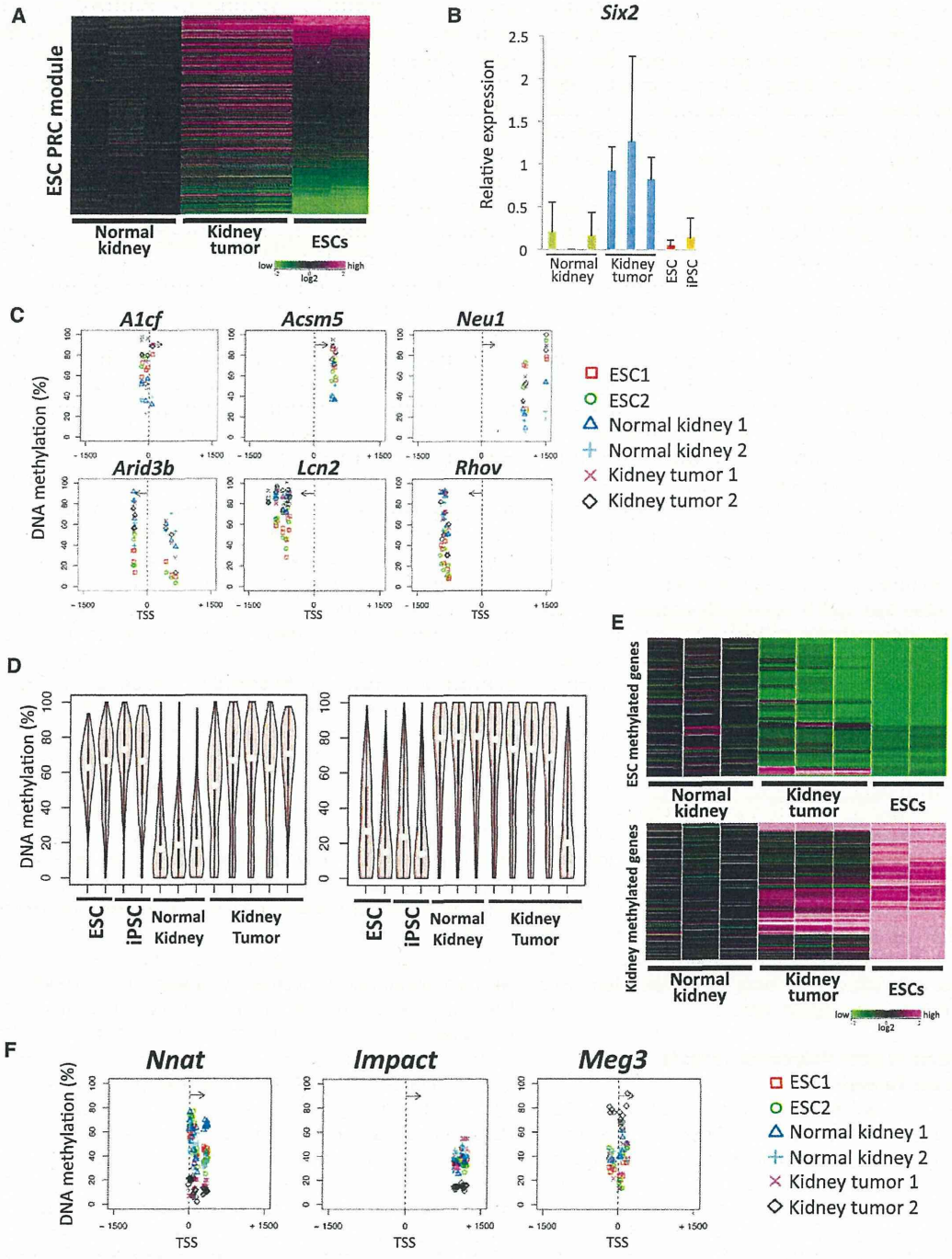

Figure 4. Altered Epigenetic Regulation in Dox-Withdrawn Tumors

(A) The microarray analyses revealed that ESC-PRC target genes were often activated in Dox-withdrawn kidney tumors compared to normal kidney tissues.

(B) *Six2* was highly expressed only in the Dox-withdrawn kidney tumors. Data are presented as mean ± SD. The mean level of kidney tumors was set to 1.

(C) Altered DNA methylation patterns in Dox-withdrawn tumors and the DNA methylation status of representative genes in the RRBS analyses.

(D) The global analyses for the DNA methylation levels. Genes that were differentially methylated between ESCs and normal kidney samples (more than 30% difference) were extracted and then analyzed for DNA methylation levels in Dox-withdrawn kidney tumors. Kidney tumors gain DNA methylation at ESC-methylated genes, whereas kidney-methylated genes often retain their methylation status in kidney tumors.

(legend continued on next page)

program, which is affected in part by the cell of origin (Figure S5A).

Altered DNA Methylation in Dox-Withdrawn Kidney Tumor Cells

Somatic cell reprogramming is accompanied by global changes in DNA methylation patterns (Mikkelsen et al., 2008). The fact that failed reprogramming can cause tumor development suggests that altered epigenetic modifications play a role in tumorigenesis. To quantitatively profile DNA methylation in Dox-withdrawn tumors, we next performed reduced representation bisulfite sequencing (RRBS) (Meissner et al., 2005). We identified a number of genes with altered DNA methylation levels in Dox-withdrawn tumors as compared to normal kidney tissues. Dox-withdrawn tumors revealed frequent gains of DNA methylation at DNA-methylated genes in ESCs, whereas loss of methylation at DNA-methylated genes in kidney tissues was not evident (Figure 4C). To validate these findings, we next performed a global analysis. We first extracted genes differentially methylated between ESCs and normal kidney samples and then examined their DNA methylation in Dox-withdrawn tumors. The global analysis confirmed that Dox-withdrawn kidney tumors gained de novo methylation at ESC-methylated genes, whereas kidney-methylated genes often retain their methylation in Dox-withdrawn kidney tumors (Figure 4D). Consistent with these findings, ESC-methylated genes were frequently found to be repressed in Dox-withdrawn tumors, whereas kidney-methylated genes tended to remain silent in these tumors (Figure 4E). These results suggest that loss of somatic cell-specific DNA methylation is preceded by a gain of ESC-specific DNA methylation patterns during the reprogramming process.

Adult cancers generally exhibit two distinct patterns of alterations in DNA methylation: site-specific DNA hypermethylation and global DNA hypomethylation (Jones and Baylin, 2002; Yamada et al., 2005). We performed specified regional analyses for the DNA methylation in normal kidney tissues and Dox-withdrawn kidney tumors. DNA hypermethylation at promoter regions in Dox-withdrawn tumors was not detectable, regardless of the presence of CpG islands (Figure S5B). Additionally, decreased DNA methylation levels at intergenic regions were not obvious in Dox-withdrawn tumors (Figure S5B).

We found that Dox-withdrawn kidney tumors aberrantly express a number of imprinted genes and that altered expression levels are similar to those in ESCs (Figure S5C). When DNA methylation status at differentially methylated regions (DMRs) of imprinted genes were examined in Dox-withdrawn tumors using a MassARRAY platform (Ehrich et al., 2005), we found frequent alterations of DNA methylation status at DMRs in Dox-withdrawn tumors (Figure S5D). The aberrant genomic methylation levels at imprinted genes in Dox-withdrawn tumors were also confirmed by RRBS analysis (Figures 4F and S5E). Intriguingly, each Dox-withdrawn tumor revealed variable aberrations in DNA methylation at different imprinted genes. The aberrant methylation includes hypermethylation at the *Meg3* (*Gtl2*) DMR, which has been correlated with impaired differentiation properties of iPSCs (Stadtfeld et al., 2010a) (Figures 4F and S5E). Moreover, SNP analysis in the hybrid KH2 background revealed that the altered expression of some imprinted genes in Dox-withdrawn tumors arise from biallelic transcription, compared to monoallelic expression in the original OSKM-inducible ESCs (Figure S5F). Collectively, these results suggest that genomic imprinting is unstable in Dox-withdrawn tumors and provide additional evidence that altered gene expression underlying tumor development is associated with altered epigenetic signatures.

Dox-Withdrawn Kidney Tumors Resemble Wilms Tumors

Histological analysis revealed that Dox-withdrawn kidney tumors in reprogrammable mice resemble Wilms tumor, the most common pediatric kidney cancer (Figure 5A). A number of studies demonstrated that increased expression of *Igf2* with DNA hypermethylation at the *H19* DMR is one of the causative and most common alterations in Wilms tumors (Ogawa et al., 1993; Steenman et al., 1994). We confirmed that Dox-withdrawn tumors express a significantly higher level of *Igf2* than noninduced tissues (Figures 5B and S6A). Moreover, consistent with altered DNA methylation at other imprinted genes, the increased methylation at the *H19* DMR was detectable in some Dox-withdrawn kidney tumors (Figure 5C).

To additionally evaluate the similarity between Dox-withdrawn kidney tumors and Wilms tumors, we next compared global gene expression patterns. We first selected genes that are upregulated more than 5-fold in Dox-withdrawn kidney tumors in comparison with noninduced kidney tissues and then assessed expression of their human orthologs in human normal kidney tissues, Wilms tumors, and human ESCs (hESCs) using previously reported microarray data sets (Tchieu et al., 2010; Yusenko et al., 2009). We found that upregulated genes in Dox-withdrawn kidney tumors are frequently upregulated in both Wilms tumors and hESCs as compared to normal kidney samples (Figure 5D), whereas this upregulation is not evident in adult kidney cancers (renal cell carcinomas [RCCs]) (Figure S6B).

We also analyzed the expression of genes in ESC-Core, ESC-Myc, and ESC-PRC modules in Wilms tumors. Notably, ESC-upregulated genes in both ESC-Core and ESC-Myc modules are similarly activated in Wilms tumors (Figures 5D and S6C), although *NANOG* and *OCT3/4* are not expressed in Wilms tumors. In contrast, a fraction of ESC-PRC targeted genes expressed in kidney progenitors, such as *SIX2* and *LGR5*, are specifically upregulated in Wilms tumors as compared with

(E) DNA-methylation-associated gene regulation in Dox-withdrawn tumors. The vast majority of ESC-methylated genes were downregulated in Dox-withdrawn tumors, whereas a significant portion of kidney-methylated genes remained repressed in these tumors. ESC-methylated genes with decreased expression levels in ESCs and kidney-methylated genes with decreased expression levels in the kidney tissues were examined.

(F) Altered DNA methylation at the DMR of imprinting genes. Note that kidney tumor 2 showed aberrant methylation patterns at *Nnat*, *Impact*, and *Meg3*. In contrast, kidney tumor 1 showed an aberration only at *Nnat*.

See also Figures S4 and S5.

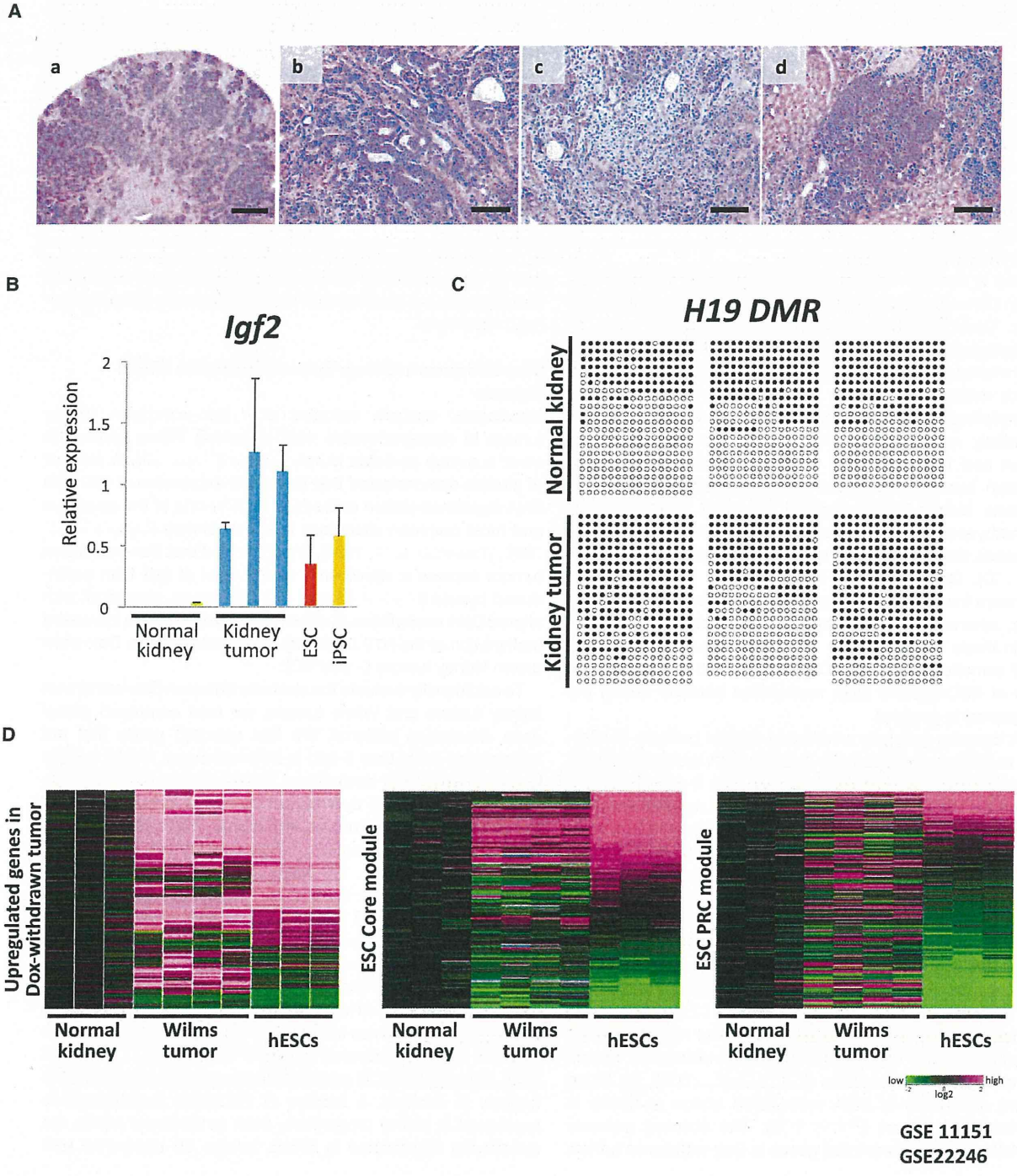

Figure 5. Dox-Withdrawn Kidney Tumors Resemble Wilms Tumors

(A) Representative histological findings of Dox-withdrawn kidney tumors (a–d). Tumors consisted of epithelial (b), stromal (c), and blastema-like (d) compartments, which are histological features of Wilms tumors. Scale bars, 500 μm (a) and 100 μm (b–d).

(B) The results of the qRT-PCR analysis for *Igf2*. *Igf2* was highly expressed in Dox-withdrawn kidney tumors. Data are presented as mean ± SD. The mean level of kidney tumors was set to 1.

(legend continued on next page)

those in normal kidney tissues, hESCs, and RCCs (Figures 5D and S6D) (Aiden et al., 2010). Collectively, kidney tumors induced by the transient expression of reprogramming factors display a number of shared characteristics with Wilms tumor. These findings also indicate that our mouse model may prove useful to uncover the pathogenesis of Wilms tumors.

iPSCs Derived from Dox-Withdrawn Kidney Tumors Contribute to Nonneoplastic Kidney Tissues in Chimeric Mice

We next tried to establish iPSCs from Dox-withdrawn kidney tumor cells. The tumor cell-specific *Lgr5-EGFP* reporter allele defined in this study was utilized to isolate tumor cells (Figures 3D, 3E, and S3E). *Lgr5*-expressing GFP-positive tumor cells were sorted and cultured in vitro with Dox to establish iPSCs from tumor cells (Figure 6A). During the culture of *Lgr5*-expressing tumor cells in vitro, *Nanog* expression at a level comparable to that in pluripotent stem cells was detected as early as 7 days after reprogramming factor induction (Figure 6B), a rate faster than the reprogramming process from normal kidney tubule cells in vitro (Figure S7A). After 2 weeks of culture with Dox exposure, more than 20 alkaline phosphatase (AP)-positive iPSC-like colonies were obtained from 100 *Lgr5*-expressing tumor cells (Figure S7B). We were able to establish Dox-independent iPSC lines from tumor cells at 3 weeks after transgene induction (Figure 6C), suggesting that the Dox-withdrawn tumor cells can be readily reprogrammed into pluripotent stem cells.

Cancers are believed to arise through the accumulation of multiple genetic abnormalities. We next investigated whether genetic abnormalities mandate the emergence of in Dox-withdrawn tumors. Exonic regions of 514 genes that include human-cancer-related genes in transplanted secondary kidney tumors were sequenced using a hybridization selection technique combined with next-generation sequencing (Table S3). Mutations in *Wt1*, *Wtx*, *Ctnnb1*, and *Trp53*, all of which have been identified in a subset of Wilms tumors, were not detected in three tumors examined. In addition, no cancer-related gene mutations were enriched in these tumors (data not shown). Array-based comparative genomic hybridization (CGH) revealed no prevalent chromosomal alteration in tumor samples (Figure S7C).

Finally, we injected the tumor-derived iPSCs into blastocysts to generate chimeric mice. Tumor-derived iPSCs contributed into adult chimeric mice (Figure 6D). Notably, the kidney-tumor-derived iPSCs differentiated into normal-looking kidney tissues (Figures 6E, 6F, and S7D). Moreover, these chimeric mice did not develop tumors even at 24 weeks of age (n = 8). To further demonstrate that tumorigenic cells can be reprogrammed into nonneoplastic cells, we also established iPSCs from the transplanted secondary tumors and confirmed their contribution to nonneoplastic kidney tissues (Figure S7E). These results substantiate that a genetic context of the Dox-withdrawn kidney tumor cells is not determinant of the cancer phenotype and support the conclusion that altered epigenetic regulations cause the abnormal growth in somatic cells, leading to the development of Dox-withdrawn tumors.

DISCUSSION

During somatic cell reprogramming, iPSCs gain the capacity for unlimited growth without particular genetic alterations. Using abbreviated reprogramming factor expression in vivo, we demonstrate that transient expression of reprogramming factors leads to tumor development. Such tumors display altered epigenetic modifications, indicating that epigenetic regulation characteristic of cellular reprogramming may also confer neoplastic growth properties to somatic cells. Intriguingly, Dox-withdrawn tumor cells are readily reprogrammed into pluripotent stem cells by additional 4F expression, indicating that the tumor cells represent a cellular state closer to iPSCs than the original somatic cells. Moreover, kidney tumor cell-derived iPSCs contribute to various somatic cell types and give rise to nonneoplastic kidney cells in mice. These data demonstrate that the abnormal growth of unsuccessfully reprogrammed cells depends predominantly on epigenetic regulations and raise the possibility that particular types of cancer may arise exclusively through altered epigenetic regulation.

Histological features of Dox-withdrawn tumors imply that unsuccessfully reprogrammed cells lack the ability to terminal differentiate along multiple lineages. It is noteworthy that Dox-withdrawn tumor cells fail to repress ESC-PRC targets yet share the activation of ESC core regulatory circuitry and Myc-related genes with pluripotent stem cells. It is conceivable that the repression of ESC-PRC targets would be exclusively associated with the acquisition of pluripotency, whereas activation of ESC core regulatory circuitry and Myc targets lead to self-renewing activity. This notion is also consistent with previous findings that PRC components are important for successful reprogramming in humans (Onder et al., 2012). Notably, the failed repression of the ESC-PRC module was detectable in previously reported partially reprogrammed cells in vitro (Polo et al., 2012), in which the activation of both ESC-Core and ESC-Myc modules had already occurred (Figure S7F). We also found that unsuccessfully reprogrammed kidney cells tend to retain DNA methylation at kidney-specific methylated genes. Considering that global epigenetic reorganization, including changes in both H3K27 methylation and DNA methylation, occurs during the later phase of iPSC generation (Polo et al., 2012), the expected repression of ESC-PRC targets and demethylation of somatic cell-specific genomic methylation might play a role in the final stages of successful somatic cell reprogramming.

Recently, Abad et al. reported that in vivo reprogramming allows the acquisition of totipotent features resulting in embryo-like cyst formation in reprogrammable mice (Abad et al., 2013). However, in the present study, we did not observe such cystic structures in Dox-treated reprogrammable mice.

(C) The bisulfite sequencing analysis revealed increased DNA methylation levels at the *H19* DMR containing two CTCF binding sites in Dox-withdrawn tumors. (D) The results of the global expression analyses in Wilms tumors. The human orthologs of upregulated genes in Dox-withdrawn tumors and ESC module genes were assessed using previously reported microarray data sets (GSE11151 and GSE22246).
See also Figure S6.

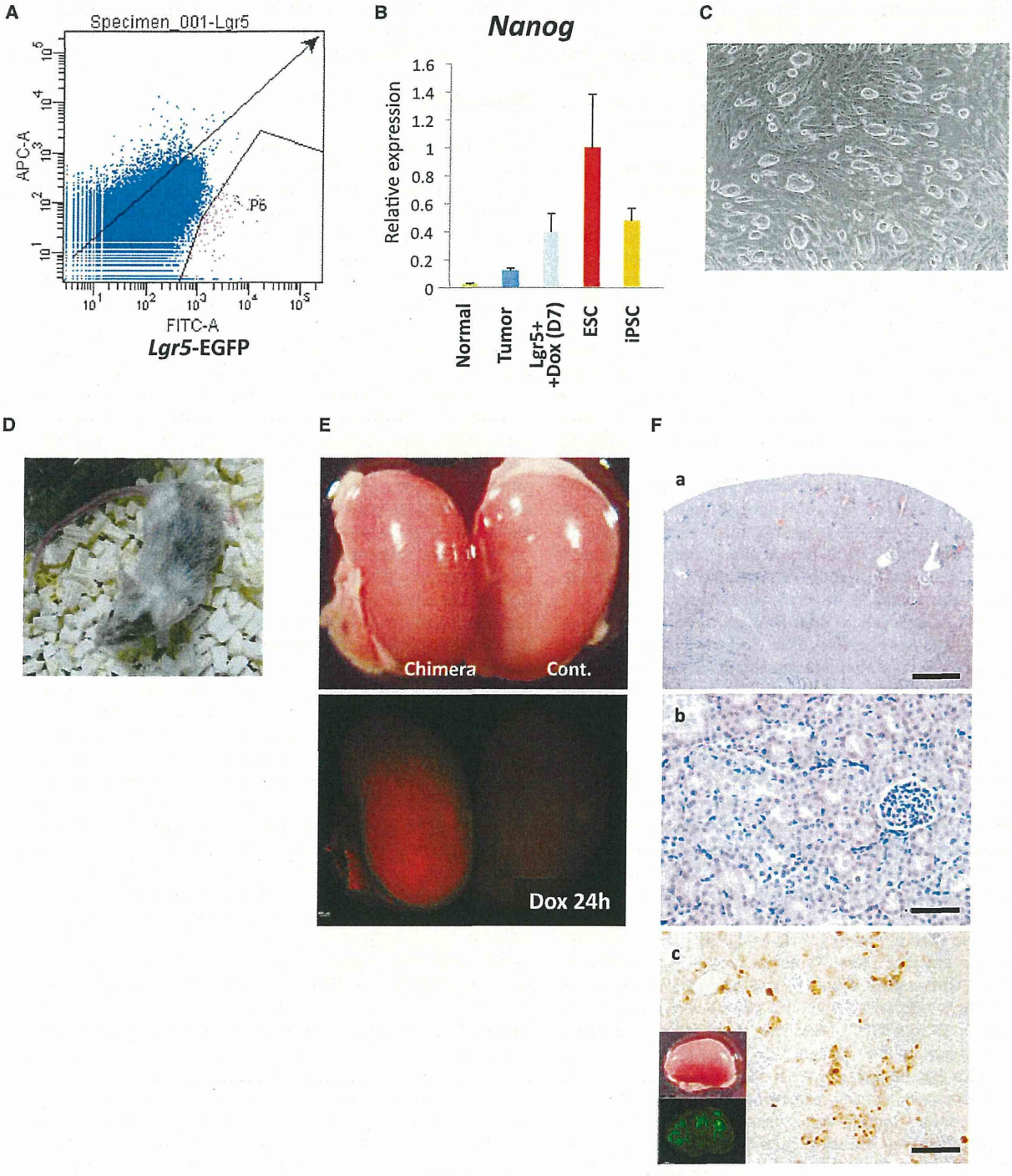

Figure 6. Generation of iPSCs from Dox-Withdrawn Tumors and Their Contribution to Normal-Looking Kidney Tissue

(A) The fluorescence-activated cell sorting analyses of Dox-withdrawn kidney tumor cells in a reprogrammable chimeric mouse with the *Lgr5*-EGFP reporter. GFP-positive *Lgr5*-expressing cells were sorted to exclusively isolate Dox-withdrawn tumor cells.

(B) Dox treatment of *Lgr5*-expressing tumor cells caused the rapid induction of *Nanog*. The *Nanog* levels were examined after seven days of treatment with Dox in vitro. Data are presented as mean ± SD. The level in ESCs was set to 1.

(C) An image of iPSCs derived from *Lgr5*-positive kidney tumor cells.

(legend continued on next page)

Furthermore, teratoma-derived in vivo iPSCs in this study failed to differentiate into placental tissues despite robust fetal contribution upon injection into eight-cell-stage embryos (data not shown), suggesting that not all in vivo iPSCs are totipotent. Because the previous study was conducted using circulating iPSCs recovered in blood, the cell of origin for in vivo reprogramming might affect the acquisition of totipotent features. It should be also noted that Abad et al. utilized germline-transmitted transgenic mice that harbor lentivirus-mediated integration of inducible reprogramming factors (Carey et al., 2009) whereas we examined chimeric mice with transgenes at a targeted locus. The different levels of transgene induction caused by such distinct transgenic systems may underlie differences in the phenotypes observed between these two studies.

Here, we show that failed reprogramming-associated cancers resemble Wilms tumors in terms of histology and molecular characteristics, including aberrant expression of imprinted genes correlated with altered DNA methylation. It is well known that Wilms tumors have characteristics distinct from adult kidney cancers in many aspects. On the basis of our findings in Dox-withdrawn tumors, we discovered that Wilms tumors harbor an activated ESC core regulatory circuitry. This is in sharp contrast to previous findings that most adult cancers do not show activation of ESC core regulatory circuitry (Kim et al., 2010). We also found that many ESC-PRC targets are not repressed in Wilms tumors, despite common repression in many cancers (Ben-Porath et al., 2008; Kim et al., 2010). Gene Ontology analysis revealed that derepressed PRC genes in Wilms tumors include genes involved in kidney development, whereas they are not enriched in derepressed PRC genes in RCCs (data not shown), suggesting that activation of the embryonic kidney transcriptional network is associated with Wilms tumor development. Taken together, strongly active ESC-core regulatory circuitry and derepression of certain ESC-PRC targets may characterize Wilms tumors and may account for the characteristics distinctive of Wilms tumors and adult kidney cancers.

Although we revealed striking similarity between Dox-withdrawn kidney tumors and Wilms tumors, it remains unclear whether reprogramming processes play a role in the development of human Wilms tumors. It has been widely accepted that nephrogenic rests, abnormally persistent clusters of embryonal cells, are the precursors of Wilms tumors. Considering the artificial expression of reprogramming factors in our experimental system, the current study does not provide direct evidence that dedifferentiation is normally involved in the human Wilms tumor development. Yet, based on our findings, it is conceivable that a reprogramming process might cause cell-fate conversion into progenitor-like states, leading to the development of nephrogenic rests required for the early stages of Wilms tumorigenesis. Further detailed analyses using human samples are required to uncover the role of reprogramming in cancer development in humans.

In summary, we demonstrated that premature termination of in vivo reprogramming causes tumor development resembling Wilms tumor. Our findings suggest that altered epigenetic regulations relating to somatic cell reprogramming drive tumorigenesis, highlighting the importance of epigenetic regulation in cancer development.

EXPERIMENTAL PROCEDURES

Generation of OSMK-Inducible ESCs

A 7 kb fragment containing Oct3/4-P2A-Sox2-T2A-Klf4-E2A-c-Myc-ires-mCherry cDNA was generated (Carey et al., 2009) and ligated into the pBS31 vector (Beard et al., 2006). The resulting construct was electroporated into KH2 ESCs to obtain OSKM-inducible ESCs (Beard et al., 2006). OKS-, KMS-, O-, LacZ-inducible ESCs were also generated using the KH2 ESCs system.

Mice

Chimeric mice were generated using reprogramming factor-inducible ESCs by diploid blastocyst injection. *Lgr5-EGFP-ires-CreERT2* mice were obtained from The Jackson Laboratory and were crossed with OSKM-inducible mice to obtain embryos. The compound transgenic MEFs were treated with Dox to establish the OSKM-inducible iPSCs with the *Lgr5-EGFP* reporter allele. All animal experiments were approved by the CiRA Animal Experiment Committee, and the care of the animals was in accordance with institutional guidelines.

Doxycycline Treatment

Mice at 4 or 14 weeks of age were administered 2 mg/ml Dox in their drinking water supplemented with 10 mg/ml sucrose. For cell culture, Dox was used at a concentration of 2 μg/ml.

Secondary Tumor Development

Primary kidney tumors were minced and treated with collagenase (1 U/ml) followed by 0.25% trypsin digestion. The dissociated tumor cells were inoculated subcutaneously into BALB/cSlc-*nu/nu* mice or C.B-17/Icr-*scid*Jcl mice to form transplanted secondary tumors.

RNA Preparation, qRT-PCR and Microarray Analysis

Total RNA was isolated using the RNeasy Plus Mini kit (QIAGEN). The quantitative real-time PCR analysis was performed using the GoTaq qPCR Master Mix (Promega). The specific primer pairs used for amplification are shown in Table S2. The transcript levels were normalized to the *β-actin* level. The microarray analysis was performed using the Mouse Gene 1.0 ST Array (Affymetrix) in accordance with the manufacturer's instructions. All of the data analyses were performed using the GeneSpring GX software program (version 12; Agilent Technology).

DNA Methylation Analyses

The RRBS analysis was performed as described previously (Boyle et al., 2012). The samples were sequenced on an Illumina HiSeq 2000 machine. Three-kilobase regions flanking transcription start site (from −1,500 to +1,500) were analyzed to examine DNA methylation levels. The DNA methylation levels for each gene were determined based on the median of DNA methylation values at CpG sites within the region. The DNA methylation values at CpG sites

(D) Kidney tumor-derived iPSCs can contribute to adult chimeric mice.
(E) No tumor formation was observed in the kidneys of chimeric mice generated with kidney tumor-derived iPSCs. Note that Dox treatment for 24 hr confirmed the contribution of kidney-tumor-derived iPSCs to the normal-looking kidney.
(F) The histological analyses of the kidneys of chimeric mice demonstrated no detectable histological abnormalities (a and b). Kidney-tumor-derived iPSCs labeled with Venus could contribute to normal-looking kidney (c). Scale bars, 500 μm (a) and 100 μm (b, c).
See also Figure S7.

containing higher than 10× coverage in all comparative samples were used for the analysis.

Histological Analysis and Immunostaining

Normal and tumor tissue samples were fixed in 10% buffered formalin for 24 hr and embedded in paraffin. Sections (4 μm) were stained with hematoxylin and eosin (H&E), and serial sections were used for the immunohistochemical analyses. The primary antibodies used were anti-Oct3/4 (1:100 dilution; BD Biosciences), anti-Ki-67 (1:100 dilution; Dako), anti-insulin (1:500 dilution; Dako), anti-BrdU (1:500 dilution; Abcam), anti-2A (1:250 dilution; Millipore), anti-Lin28b (1:100 dilution; Cell Signaling Technology), and anti-GFP (1:500 dilution; Invitrogen).

ACCESSION NUMBERS

The Gene Expression Omnibus accession number for the microarray and RRBS data reported in this paper is GSE52304.

SUPPLEMENTAL INFORMATION

Supplemental Information includes Extended Experimental Procedures, seven figures, and three tables and can be found with this article online at http://dx.doi.org/10.1016/j.cell.2014.01.005.

ACKNOWLEDGMENTS

We are grateful to T. Taya for CGH analysis and S. Sakurai and T. Sato for RRBS analysis. We also thank S. Masui, H. Sakurai, and members in Yamada laboratory for helpful discussions and T. Ukai, K. Osugi, and N. Nishimoto for assistance. The authors were supported in part by a Grant-in-Aid from the Ministry of Education, Culture, Sports, Science, and Technology of Japan (MEXT); the Ministry of Health, Labor, and Welfare of Japan; the JST; the Funding Program for World-Leading Innovative R&D on Science and Technology (FIRST Program) of the Japanese Society for the Promotion of Science (JSPS); the Takeda Science Foundation; and the Naito Foundation. S.Y. is a member without salary of the scientific advisory boards of iPierian, iPS Academia Japan, Megakaryon Corporation, and HEALIOS K. K. Japan. The iCeMS is supported by World Premier International Research Center Initiative, MEXT, Japan.

Received: May 29, 2013
Revised: November 6, 2013
Accepted: January 3, 2014
Published: February 13, 2014

REFERENCES

Abad, M., Mosteiro, L., Pantoja, C., Cañamero, M., Rayon, T., Ors, I., Graña, O., Megías, D., Domínguez, O., Martínez, D., et al. (2013). Reprogramming in vivo produces teratomas and iPS cells with totipotency features. Nature *502*, 340–345.

Aiden, A.P., Rivera, M.N., Rheinbay, E., Ku, M., Coffman, E.J., Truong, T.T., Vargas, S.O., Lander, E.S., Haber, D.A., and Bernstein, B.E. (2010). Wilms tumor chromatin profiles highlight stem cell properties and a renal developmental network. Cell Stem Cell *6*, 591–602.

Barker, N., van Es, J.H., Kuipers, J., Kujala, P., van den Born, M., Cozijnsen, M., Haegebarth, A., Korving, J., Begthel, H., Peters, P.J., and Clevers, H. (2007). Identification of stem cells in small intestine and colon by marker gene Lgr5. Nature *449*, 1003–1007.

Barker, N., Rookmaaker, M.B., Kujala, P., Ng, A., Leushacke, M., Snippert, H., van de Wetering, M., Tan, S., Van Es, J.H., Huch, M., et al. (2012). Lgr5(+ve) stem/progenitor cells contribute to nephron formation during kidney development. Cell Rep. *2*, 540–552.

Beard, C., Hochedlinger, K., Plath, K., Wutz, A., and Jaenisch, R. (2006). Efficient method to generate single-copy transgenic mice by site-specific integration in embryonic stem cells. Genesis *44*, 23–28.

Ben-Porath, I., Thomson, M.W., Carey, V.J., Ge, R., Bell, G.W., Regev, A., and Weinberg, R.A. (2008). An embryonic stem cell-like gene expression signature in poorly differentiated aggressive human tumors. Nat. Genet. *40*, 499–507.

Boyle, P., Clement, K., Gu, H., Smith, Z.D., Ziller, M., Fostel, J.L., Holmes, L., Meldrim, J., Kelley, F., Gnirke, A., and Meissner, A. (2012). Gel-free multiplexed reduced representation bisulfite sequencing for large-scale DNA methylation profiling. Genome Biol. *13*, R92.

Brambrink, T., Foreman, R., Welstead, G.G., Lengner, C.J., Wernig, M., Suh, H., and Jaenisch, R. (2008). Sequential expression of pluripotency markers during direct reprogramming of mouse somatic cells. Cell Stem Cell *2*, 151–159.

Carey, B.W., Markoulaki, S., Hanna, J., Saha, K., Gao, Q., Mitalipova, M., and Jaenisch, R. (2009). Reprogramming of murine and human somatic cells using a single polycistronic vector. Proc. Natl. Acad. Sci. USA *106*, 157–162.

Carey, B.W., Markoulaki, S., Beard, C., Hanna, J., and Jaenisch, R. (2010). Single-gene transgenic mouse strains for reprogramming adult somatic cells. Nat. Methods *7*, 56–59.

Ehrich, M., Nelson, M.R., Stanssens, P., Zabeau, M., Liloglou, T., Xinarianos, G., Cantor, C.R., Field, J.K., and van den Boom, D. (2005). Quantitative high-throughput analysis of DNA methylation patterns by base-specific cleavage and mass spectrometry. Proc. Natl. Acad. Sci. USA *102*, 15785–15790.

Folmes, C.D., Nelson, T.J., Martinez-Fernandez, A., Arrell, D.K., Lindor, J.Z., Dzeja, P.P., Ikeda, Y., Perez-Terzic, C., and Terzic, A. (2011). Somatic oxidative bioenergetics transitions into pluripotency-dependent glycolysis to facilitate nuclear reprogramming. Cell Metab. *14*, 264–271.

Fussner, E., Djuric, U., Strauss, M., Hotta, A., Perez-Iratxeta, C., Lanner, F., Dilworth, F.J., Ellis, J., and Bazett-Jones, D.P. (2011). Constitutive heterochromatin reorganization during somatic cell reprogramming. EMBO J. *30*, 1778–1789.

Hochedlinger, K., Yamada, Y., Beard, C., and Jaenisch, R. (2005). Ectopic expression of Oct-4 blocks progenitor-cell differentiation and causes dysplasia in epithelial tissues. Cell *121*, 465–477.

Hong, H., Takahashi, K., Ichisaka, T., Aoi, T., Kanagawa, O., Nakagawa, M., Okita, K., and Yamanaka, S. (2009). Suppression of induced pluripotent stem cell generation by the p53-p21 pathway. Nature *460*, 1132–1135.

Jones, P.A., and Baylin, S.B. (2002). The fundamental role of epigenetic events in cancer. Nat. Rev. Genet. *3*, 415–428.

Kim, J., Woo, A.J., Chu, J., Snow, J.W., Fujiwara, Y., Kim, C.G., Cantor, A.B., and Orkin, S.H. (2010). A Myc network accounts for similarities between embryonic stem and cancer cell transcription programs. Cell *143*, 313–324.

Kobayashi, A., Valerius, M.T., Mugford, J.W., Carroll, T.J., Self, M., Oliver, G., and McMahon, A.P. (2008). Six2 defines and regulates a multipotent self-renewing nephron progenitor population throughout mammalian kidney development. Cell Stem Cell *3*, 169–181.

Maherali, N., Sridharan, R., Xie, W., Utikal, J., Eminli, S., Arnold, K., Stadtfeld, M., Yachechko, R., Tchieu, J., Jaenisch, R., et al. (2007). Directly reprogrammed fibroblasts show global epigenetic remodeling and widespread tissue contribution. Cell Stem Cell *1*, 55–70.

Meissner, A., Gnirke, A., Bell, G.W., Ramsahoye, B., Lander, E.S., and Jaenisch, R. (2005). Reduced representation bisulfite sequencing for comparative high-resolution DNA methylation analysis. Nucleic Acids Res. *33*, 5868–5877.

Mikkelsen, T.S., Ku, M., Jaffe, D.B., Issac, B., Lieberman, E., Giannoukos, G., Alvarez, P., Brockman, W., Kim, T.K., Koche, R.P., et al. (2007). Genome-wide maps of chromatin state in pluripotent and lineage-committed cells. Nature *448*, 553–560.

Mikkelsen, T.S., Hanna, J., Zhang, X., Ku, M., Wernig, M., Schorderet, P., Bernstein, B.E., Jaenisch, R., Lander, E.S., and Meissner, A. (2008). Dissecting direct reprogramming through integrative genomic analysis. Nature *454*, 49–55.

Ogawa, O., Eccles, M.R., Szeto, J., McNoe, L.A., Yun, K., Maw, M.A., Smith, P.J., and Reeve, A.E. (1993). Relaxation of insulin-like growth factor II gene imprinting implicated in Wilms' tumour. Nature *362*, 749–751.

Ohta, S., Nishida, E., Yamanaka, S., and Yamamoto, T. (2013). Global splicing pattern reversion during somatic cell reprogramming. Cell Rep. *5*, 357–366.

Okita, K., Ichisaka, T., and Yamanaka, S. (2007). Generation of germline-competent induced pluripotent stem cells. Nature *448*, 313–317.

Onder, T.T., Kara, N., Cherry, A., Sinha, A.U., Zhu, N., Bernt, K.M., Cahan, P., Marcarci, B.O., Unternaehrer, J., Gupta, P.B., et al. (2012). Chromatin-modifying enzymes as modulators of reprogramming. Nature *483*, 598–602.

Polo, J.M., Anderssen, E., Walsh, R.M., Schwarz, B.A., Nefzger, C.M., Lim, S.M., Borkent, M., Apostolou, E., Alaei, S., Cloutier, J., et al. (2012). A molecular roadmap of reprogramming somatic cells into iPS cells. Cell *151*, 1617–1632.

Rais, Y., Zviran, A., Geula, S., Gafni, O., Chomsky, E., Viukov, S., Mansour, A.A., Caspi, I., Krupalnik, V., Zerbib, M., et al. (2013). Deterministic direct reprogramming of somatic cells to pluripotency. Nature *502*, 65–70.

Samavarchi-Tehrani, P., Golipour, A., David, L., Sung, H.K., Beyer, T.A., Datti, A., Woltjen, K., Nagy, A., and Wrana, J.L. (2010). Functional genomics reveals a BMP-driven mesenchymal-to-epithelial transition in the initiation of somatic cell reprogramming. Cell Stem Cell *7*, 64–77.

Sridharan, R., Tchieu, J., Mason, M.J., Yachechko, R., Kuoy, E., Horvath, S., Zhou, Q., and Plath, K. (2009). Role of the murine reprogramming factors in the induction of pluripotency. Cell *136*, 364–377.

Stadtfeld, M., Apostolou, E., Akutsu, H., Fukuda, A., Follett, P., Natesan, S., Kono, T., Shioda, T., and Hochedlinger, K. (2010a). Aberrant silencing of imprinted genes on chromosome 12qF1 in mouse induced pluripotent stem cells. Nature *465*, 175–181.

Stadtfeld, M., Maherali, N., Borkent, M., and Hochedlinger, K. (2010b). A reprogrammable mouse strain from gene-targeted embryonic stem cells. Nat. Methods *7*, 53–55.

Steenman, M.J., Rainier, S., Dobry, C.J., Grundy, P., Horon, I.L., and Feinberg, A.P. (1994). Loss of imprinting of IGF2 is linked to reduced expression and abnormal methylation of H19 in Wilms' tumour. Nat. Genet. *7*, 433–439.

Takahashi, K., and Yamanaka, S. (2006). Induction of pluripotent stem cells from mouse embryonic and adult fibroblast cultures by defined factors. Cell *126*, 663–676.

Takahashi, K., Tanabe, K., Ohnuki, M., Narita, M., Ichisaka, T., Tomoda, K., and Yamanaka, S. (2007). Induction of pluripotent stem cells from adult human fibroblasts by defined factors. Cell *131*, 861–872.

Tchieu, J., Kuoy, E., Chin, M.H., Trinh, H., Patterson, M., Sherman, S.P., Aimiuwu, O., Lindgren, A., Hakimian, S., Zack, J.A., et al. (2010). Female human iPSCs retain an inactive X chromosome. Cell Stem Cell *7*, 329–342.

Wernig, M., Meissner, A., Foreman, R., Brambrink, T., Ku, M., Hochedlinger, K., Bernstein, B.E., and Jaenisch, R. (2007). In vitro reprogramming of fibroblasts into a pluripotent ES-cell-like state. Nature *448*, 318–324.

Woltjen, K., Michael, I.P., Mohseni, P., Desai, R., Mileikovsky, M., Hämäläinen, R., Cowling, R., Wang, W., Liu, P., Gertsenstein, M., et al. (2009). piggyBac transposition reprograms fibroblasts to induced pluripotent stem cells. Nature *458*, 766–770.

Yamada, Y., Jackson-Grusby, L., Linhart, H., Meissner, A., Eden, A., Lin, H., and Jaenisch, R. (2005). Opposing effects of DNA hypomethylation on intestinal and liver carcinogenesis. Proc. Natl. Acad. Sci. USA *102*, 13580–13585.

Yusenko, M.V., Kuiper, R.P., Boethe, T., Ljungberg, B., van Kessel, A.G., and Kovacs, G. (2009). High-resolution DNA copy number and gene expression analyses distinguish chromophobe renal cell carcinomas and renal oncocytomas. BMC Cancer *9*, 152.

Development 140, 66-75 (2013) doi:10.1242/dev.084103

Dose-dependent roles for canonical Wnt signalling in *de novo* crypt formation and cell cycle properties of the colonic epithelium

Akihiro Hirata[1,*], Jochen Utikal[2,3,*], Satoshi Yamashita[4], Hitomi Aoki[5], Akira Watanabe[6], Takuya Yamamoto[6], Hideyuki Okano[7], Nabeel Bardeesy[2], Takahiro Kunisada[5], Toshikazu Ushijima[4], Akira Hara[8], Rudolf Jaenisch[9], Konrad Hochedlinger[2,‡] and Yasuhiro Yamada[6,10,‡]

SUMMARY

There is a gradient of β-catenin expression along the colonic crypt axis with the highest levels at the crypt bottom. In addition, colorectal cancers show a heterogeneous subcellular pattern of β-catenin accumulation. However, it remains unclear whether different levels of Wnt signalling exert distinct roles in the colonic epithelium. Here, we investigated the dose-dependent effect of canonical Wnt activation on colonic epithelial differentiation by controlling the expression levels of stabilised β-catenin using a doxycycline-inducible transgenic system in mice. We show that elevated levels of Wnt signalling induce the amplification of Lgr5+ cells, which is accompanied by crypt fission and a reduction in cell proliferation among progenitor cells. By contrast, lower levels of β-catenin induction enhance cell proliferation rates of epithelial progenitors without affecting crypt fission rates. Notably, slow-cycling cells produced by β-catenin activation exhibit activation of Notch signalling. Consistent with the interpretation that the combination of Notch and Wnt signalling maintains crypt cells in a low proliferative state, the treatment of β-catenin-expressing mice with a Notch inhibitor turned such slow-cycling cells into actively proliferating cells. Our results indicate that the activation of the canonical Wnt signalling pathway is sufficient for *de novo* crypt formation, and suggest that different levels of canonical Wnt activations, in cooperation with Notch signalling, establish a hierarchy of slower-cycling stem cells and faster-cycling progenitor cells characteristic for the colonic epithelium.

KEY WORDS: Wnt signalling, Notch signalling, Intestinal stem cell, Mouse

INTRODUCTION

The intestinal epithelium is characterised by rapid and continuous renewal throughout life. One of the major players involved in the renewal of the intestinal epithelium is the canonical Wnt signalling pathway. Experimental manipulation of Wnt signalling has been shown to influence epithelial proliferation in the intestines (Korinek et al., 1998; Pinto et al., 2003; Kuhnert et al., 2004; Sansom et al., 2004; Andreu et al., 2005; Fevr et al., 2007). For example, inactivation of Wnt signalling by transgenic or adenoviral expression of *Dickkopf1* (*Dkk1*), a secreted Wnt inhibitor, leads to marked inhibition of epithelial proliferation in the intestines (Pinto et al., 2003; Kuhnert et al., 2004). By contrast, two independent groups have demonstrated that loss of *Apc* results in a rapid and dramatic enlargement of the crypt compartment associated with abnormal cell proliferation in the small intestine (Sansom et al., 2004; Andreu et al., 2005). Together, these experiments provide definitive evidence for the importance of Wnt signalling in controlling intestinal epithelial proliferation.

In addition to controlling cell proliferation, a role for Wnt/β-catenin signalling in stem cell maintenance in the intestine has been suggested. Inactivation of Wnt signalling by either overexpression of *Dkk1* or conditional deletion of *Ctnnb1* (the gene encoding β-catenin) results in the loss of intestinal crypts, indicating that Wnt signalling is indispensable for stem cell maintenance (Pinto et al., 2003; Kuhnert et al., 2004; Fevr et al., 2007). In fact, the intestinal stem cell (ISC) marker *Lgr5* has initially been identified as a target of β-catenin/Tcf transcription (Barker et al., 2007), which is in accordance with the view that ISCs harbour a higher activity of canonical Wnt signals. In further support of this notion, nuclear accumulation of β-catenin has been observed at the crypt bottom in cells that potentially include ISCs (van de Wetering et al., 2002).

The number of ISCs has to be tightly regulated in the intestinal crypts in order to facilitate tissue turnover but prevent abnormal growth. ISCs are usually involved in a process of homeostatic self-renewal in the adult intestine but can also be rapidly recruited to repair tissues after injury. Indirect evidence for an involvement of Wnt signalling in stem cell amplification derives from a study showing that PTEN deficiency increases the frequency of crypt fission/budding and the number of cells expressing *Musashi1*, a putative ISC marker, through activated Wnt signalling (He et al., 2007). However, the underlying mechanism by which activated Wnt signalling may expand ISCs remains elusive, and direct evidence

[1]Division of Animal Experiment, Life Science Research Center, Gifu University, 1-1 Yanagido, Gifu, 501-1194, Japan. [2]Massachusetts General Hospital Cancer Center and Center for Regenerative Medicine, Harvard Stem Cell Institute, 185 Cambridge Street, Boston, MA 02114, USA. [3]Skin Cancer Unit, German Cancer Research Center, Heidelberg, Germany and Department of Dermatology, Venereology and Allergology, University Medical Center Mannheim, Ruprecht-Karl University of Heidelberg, Mannheim, Germany. [4]Division of Epigenomics, National Cancer Center Research Institute, 5-1-1 Tsukiji, Chuo-ku, Tokyo, Japan. [5]Department of Tissue and Organ Development and [8] Department of Tumor Pathology, Gifu University Graduate School of Medicine, 1-1 Yanagido, Gifu, 501-1194, Japan. [6]Center for iPS Cell Research and Application (CiRA), Institute for Integrated Cell-Material Sciences (WPI-iCeMS), Kyoto University, 53 Kawahara-cho, Shogoin, Sakyo-ku, Kyoto 606-8507, Japan. [7]Department of Physiology, Keio University School of Medicine, 35 Shinanomach, Shinjuku-ku, Tokyo 160-8582, Japan. [9]Whitehead Institute for Biomedical Research, Massachusetts Institute of Technology, Cambridge, MA 02142, USA. [10]PRESTO, Japan Science and Technology Agency, Saitama, Japan.

*These authors contributed equally to this work
‡Authors for correspondence (khochedlinger@helix.mgh.harvard.edu; y-yamada@cira.kyoto-u.ac.jp)

Accepted 15 October 2012